

The Relationship Between Microwave Brightness Temperature, Salinity, and Thickness of Sea Ice Acquired With a Tank Experiment

Kohei Cho^{ID}, Kazuhiro Naoki, Masashige Nakayama, and Tomonori Tanikawa^{ID}

Abstract—There is a strong need for measuring sea ice thickness with passive microwave radiometers onboard satellites. However, since the footprint size of passive microwave radiometers is 5–50 km, it is not easy to verify the possibility using satellite data. To study how the microwave brightness temperature and emissivity change with sea ice thickness and salinity, the authors have been performing a sea ice tank experiment for the past few years. The tank, which has a diameter of 2.6 m, was filled with seawater having a salinity of 32.5 ppt to a depth of 0.85 m. The tank was installed outdoors and covered with a hood to keep the surface from being covered by snow. The continuous measurement of microwave brightness temperature, salinity, and thickness of artificially grown sea ice in a tank was performed under subfreezing temperatures. The brightness temperature measurements were made at 7, 18, and 36 GHz for both vertical (V) and horizontal (H) polarizations using a portable microwave radiometer MMRS2 developed by MELOS. During the experiment, the sea ice thickness went up to 54.5 cm. The brightness temperature and emissivity measured by the portable microwave radiometer saturated at sea ice thickness of 3.0 cm for 36 GHz, 5.0 cm for 18 GHz, and 13.5 cm for 7 GHz. The relationship between PR and ice thickness as well as the relationship between GR and ice thickness were also examined. The result suggested the limitation and possibility of estimating sea ice thickness with passive microwave radiometers.

Index Terms—AMSR2, emissivity, microwave radiometer.

I. INTRODUCTION

PASSIVE microwave radiometer observation from space is one of the most powerful tools for monitoring global sea ice distribution. Ice concentration is the most fundamental parameter of sea ice, which can be calculated from brightness temperatures measured by passive microwave radiometers onboard satellites. Various ice concentration algorithms have been developed in the past, including NASA Team Algorithm

Manuscript received 25 July 2023; revised 23 October 2023, 26 December 2023, and 11 January 2024; accepted 20 January 2024. Date of publication 7 February 2024; date of current version 15 February 2024. This work was financially supported by the Japan Aerospace Exploration Agency (JAXA) Third Research Announcement on the Earth Observation under Grant EO-RA3. (*Kohei Cho, Kazuhiro Naoki, Masashige Nakayama, and Tomonori Tanikawa contributed equally to this work.*) (*Corresponding author: Kohei Cho*.)

Kohei Cho and Kazuhiro Naoki are with Tokai University Research and Information Center (TRIC), Tokyo 108-8619, Japan (e-mail: kohei.cho@tokai-u.jp; naoki.kazuhiro.k@tokai.ac.jp).

Masashige Nakayama is with the Faculty of Education, Hokkaido University of Education, Hokkaido 085-8580, Japan (e-mail: nakayama.masashige@k.hokkyodai.ac.jp).

Tomonori Tanikawa is with the Meteorological Research Institute (MRI), Japan Meteorological Agency, Tsukuba 305-0052, Japan (e-mail: tanikawa@mri-jma.go.jp).

Digital Object Identifier 10.1109/TGRS.2024.3361904

(Cavarieli et al. [1]), Bootstrap Algorithm (Comiso et al. [2], [3]), and ASI Algorithm (Spreen et al. [4]). The ice concentration calculated from the time series of passive microwave radiometer observations clarified the serious reduction trend of sea ice extent in the Northern Hemisphere (e.g., Comiso and Nishio [5], Comiso et al. [6], and Stroeve et al. [7]). The result has been used as evidence of global warming in the Sixth Assessment Report of IPCC [8]. The importance of monitoring sea ice using passive microwave radiometers from space is increasing more than ever.

Since the heat flux of ice is strongly affected by the ice thickness [9], ice thickness is another important parameter of sea ice, which is expected to be measured by passive microwave radiometers. Studies on estimating ice thickness from the brightness temperature data acquired from passive microwave radiometers onboard satellites have been performed in the past, including those of Tateyama et al. [10], Martin et al. [11], Martin and Drucker [12], Tamura et al. [13], Aulicino et al. [14], and Kashiwase et al. [15]. However, since the footprint size of passive microwave radiometers onboard satellites is usually 5–50 km, collecting truth data of ice thickness representing the ice area of 5 × 5 to 50 × 50 km is not easy. Cho et al. [16] have been comparing AMSR2 data with higher spatial resolution optical sensor data and investigated that at least a thin ice area with an ice thickness of less than around 20–30 cm could be identified with AMSR2 data. Anyway, to clarify the possibility of estimating sea ice thickness with passive microwave sensors, ground-based observation is necessary. One of the practical ways of experiment is to measure the brightness temperature of ice growing in the tank with portable microwave radiometers. Since the 1980s, various studies on microwave properties of thin ice using outdoor tanks have been performed, including Arcone et al. [17], Grenfell et al. [18], Nghiem et al. [19], Naoki et al. [20], Shokr et al. [21], and Shokr and Kaleschke [22]. Arcone et al. [17] performed an outdoor pool experiment to examine the microwave dielectric, structure, and profile of simulated sea ice. The results showed that both the real and imaginary parts of the dielectric permittivity vary almost in direct proportion to the brine volume of the simulated sea ice. Nghiem et al. [19] performed an outdoor experiment to study diurnal thermal cycling effects on microwave signatures of thin sea ice. In this experiment, the ice sheet grew from open water with a salt mixture similar to seawater to a thickness of 10 cm, and the linear relationship

between the ice thickness and bulk salinity was acquired. However, the bulk salinity of ice with a thickness of less than 2 cm was not acquired. Naoki et al. [20] performed microwave measurements of sea ice from an aircraft and compared it with ice thickness measured from a ship in the sea of Okhotsk. The results showed that the brightness temperature and emissivity increase with the thickness of thin ice for a frequency range of 10–37 GHz. The result also showed that the relationship is more pronounced at lower frequencies and horizontal polarization. Through the field experiment at Saroma Lake, it was concluded that passive microwave radiometric signals likely contain indirect information on ice thickness through the dependence of dielectric properties on brine. However, the detailed measurement for the ice thickness less than 5 cm was not performed in this experiment. Shokr et al. [21] and Shokr and Kaleschke [22] performed outdoor tank experiments, and microwave radiation was sampled for 19, 37, and 85 GHz during the growing stage of simulated thin sea ice. The results revealed that microwave radiation from thin ice is particularly sensitive to surface change due to meteorological factors such as rain, freezing rain, slash, and snowfall. Among these previous tank experiments, Grenfell et al. [18] performed a dedicated tank experiment using radiometers including frequencies of 4 to 7, 10, 18, 37, 85, and 90 GHz. The ice was grown in a tank located outdoors, and microwave brightness temperatures were continuously measured to identify how the ice-growing process could be captured by the microwave radiometer measurement. The saturation of microwave emissivity occurred at ice thicknesses of 15, 8, and 3 mm for 18, 37, and 90 GHz in the vertical polarization. As for the C-band (4–7 GHz) at horizontal polarization, the brightness temperature saturated at around 50 mm. However, the relationships between ice thickness and brightness temperature for those bands with both vertical and horizontal polarizations were not presented in their paper. These results gave us good motivation to perform our ice tank experiment.

As for the shipborne experiment, Hwang et al. [23] have investigated the microwave emission properties of newly formed sea ice. This article emphasized that microwave emissions of thin sea ice are quite different between different ice types and the existence of snow cover. In order to examine the possibility of estimating ice thickness with a passive microwave radiometer in detail, Naoki et al. [24], [25] have been performing a sea ice tank experiment using portable microwave radiometers.

II. INSTRUMENTS

A. Microwave Radiometer

A portable microwave radiometer MMRS2 of Mitsubishi Electric TOKKI Systems Company was used in this study. Fig. 1 and Table I show the outlook and specification of MMRS2, respectively. The 7.3-GHz instrument has dual-polarization (V and H) channels. For the 18.7-GHz instrument, two were used for V and H polarizations. However, since we had only one 36.5-GHz instrument with a single polarization channel, we rotated the instrument 90° to perform V- and H-polarized observation.

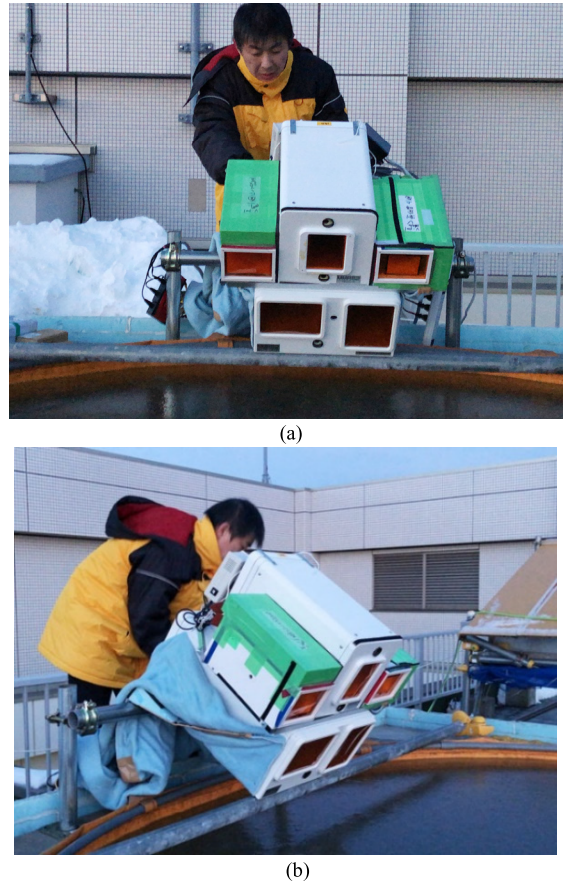


Fig. 1. Outlook of portable microwave radiometer MMRS2. (a) Front view. (b) Side view.

TABLE I
SPECIFICATIONS OF MMRS2

Parameter	Specification		
Center Frequency	7.3 GHz	18.7 GHz	36.5 GHz
Polarization	V and H		Single (V or H)
Accuracy	1 K Typ.		
Beam width	15 deg.	10 deg.	7 deg.
Incidence angle	55 deg.		

The two-point calibration was performed for the calibration of the radiometers. A noise diode is used for the high-temperature reference source and a dummy load is used for the normal-temperature reference. The 1 K accuracy is promised for 300 K.

B. Sea Ice Tank

A sea ice tank was installed outdoors on the rooftop of a seven-story building at the Hokkaido University of Education, Kushiro Campus, Hokkaido, Japan. The tank was covered with a removable hood to keep the water surface from being covered by snow. A refrigerator was attached to the hood to cool the tank from the top. The tank has a diameter of 2.6 m and was filled with seawater from the Pacific Ocean with a salinity of 32.5 ppt to a depth of 0.85 m. The side and the bottom of the tank were covered with a heat insulator. A thermometer was vertically attached to the tank to continuously measure the water temperature profile of the tank. Figs. 2 and 3 show the structure diagram and the outlook of the tank, respectively.

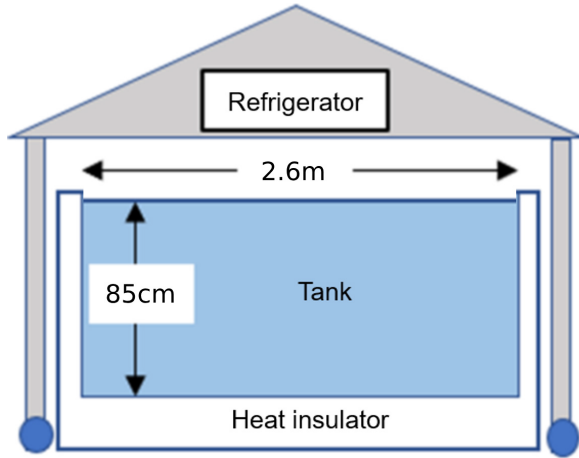


Fig. 2. Structure diagram of the sea ice tank.

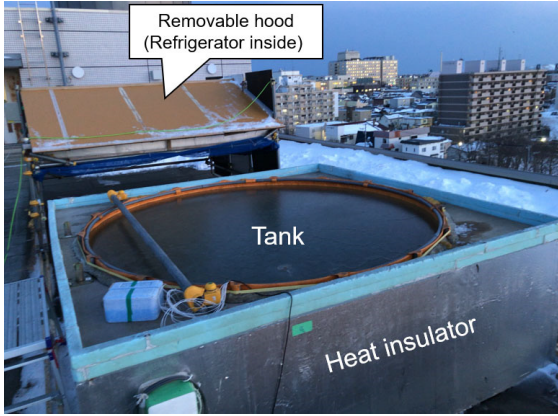


Fig. 3. Outlook of the sea ice tank.

III. MEASUREMENT PROCEDURE

The portable microwave radiometer was attached to the tank, as shown in Fig. 1(b). The tank was covered with a removable roof to avoid solar radiation and snowfall on the seawater/ice surface of the tank. On the first day of the experiment, the seawater in the tank started to freeze under no wind or no snowfall conditions and the sea ice surface was smooth. Since the roof was removed only at the time of measurement, the sea ice surface was kept smooth without snow cover all through the experiment. The measurement of the ice thickness, salinity, temperature, and brightness temperature of the surface of the sea ice layer was performed every night under subfreezing temperatures. The brightness temperature measurements were made at 7, 18, and 36 GHz for both vertical (V) and horizontal (H) polarizations using the portable microwave radiometer MMRS2. The incidence angle of the radiometer was set to 55° to be consistent with that of the microwave radiometer AMSR2 on board the GCOM-W satellite of JAXA. In our experiment, the microwave measurement was conducted at night under clear sky conditions. Therefore, the authors considered that the influence of downwelling atmospheric radiation is negligible. Measurement of ice thickness was performed one to three times a day for the first seven days by directly measuring the thickness of the ice core. Due to the limitations of the size of the ice tank, the authors could sample sea ice only for measuring the bulk salinity. In order to support the ice growth,

the tank was mostly covered with a removable hood, and the tank was continuously cooled by the refrigerator attached to the hood (see Fig. 2). At the time of microwave measurement, the hood was removed and the MMRS2 was attached to the top of the tank for measurement. The details of the instrument development and measurements are described in our latest paper [26].

IV. RESULTS

A. Brightness Temperature/Emissivity Versus Ice Thickness

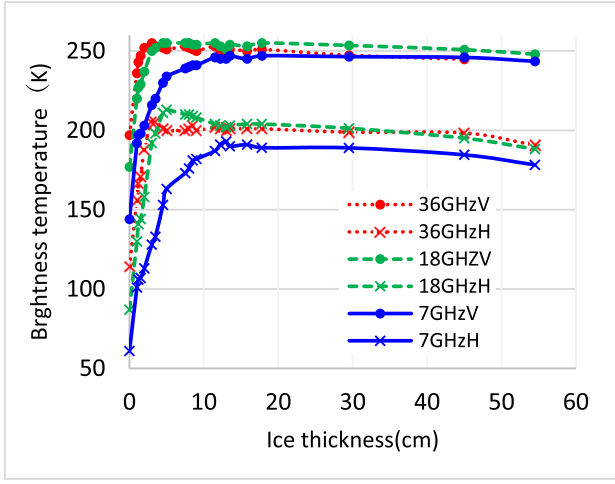
The experiment was performed for 41 days from February 4 to March 16, 2020. The microwave brightness temperature measurement and the ice thickness measurement were performed every day for the first seven days and after that with about ten-day intervals. Fig. 4 shows the result of the measurement. By introducing a refrigerator, the ice thickness went up to 54.5 cm during the experiment. The observed brightness temperature was lowest for the open water surface and increased as sea ice grew thicker. The brightness temperature at 7 GHz for V polarization reached a maximum value of 247 K when the ice thickness reached 13.5 cm and became nearly constant after that. The brightness temperature at 7 GHz for H polarization reached a maximum value of 193 K when the ice thickness reached 13.0 cm and became nearly constant after that. The brightness temperature at 18 GHz for V polarization reached a maximum value of 255 K when the ice thickness reached 4.5 cm and became nearly constant after that. The brightness temperature at 18 GHz for H polarization reached a maximum value of 213 K when the ice thickness reached 5.0 cm and became nearly constant after that. The brightness temperature at 36 GHz for V polarization reached a maximum value of 255 K when the ice thickness reached about 3.0 cm and became nearly constant after that. The brightness temperature at 36 GHz for H polarization reached a maximum value of 205 K when the ice thickness reached about 3.0 cm and became nearly constant after that. These results suggested that lower frequency has more possibility of detecting ice thickness than higher frequencies. At all three frequencies, the brightness temperature of V polarization was 40–60 K higher than H polarization usual. However, the behavior of the brightness temperature variation of both polarizations was quite similar for each frequency.

As references, the graphs of ice emissivity versus ice thickness were also plotted in Fig. 5. The ice emissivity was calculated by dividing the brightness temperature by the ice surface temperature measured by the thermistor set on the surface of the ice. The curve of each frequency in Figs. 4(b) and 5 looks almost the same reflecting the stability of the sea ice surface temperature during the experiment.

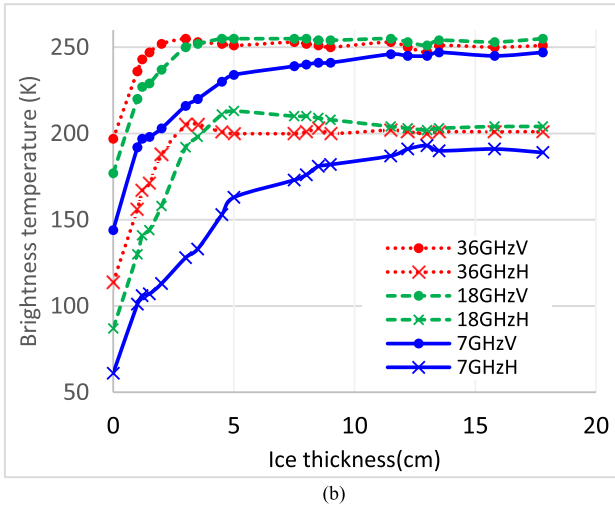
Polarization ratio (PR) and gradient ratio (GR) have been used in previous studies on extracting thin ice areas and/or estimating ice thickness from passive microwave data [10], [11], [12], [13], [14], [15]. The PR and GR can be described in the following equations:

$$PR(18 \text{ GHz}) = (TB_{18V} - TB_{18H}) / (TB_{18V} + TB_{18H}) \quad (1a)$$

where



(a)



(b)

Fig. 4. Brightness temperature versus ice thickness for 7, 18, and 36 GHz at V and H polarizations. (a) Ice thickness: 0–54.5 cm. (b) Ice thickness: 0–17.8 cm.

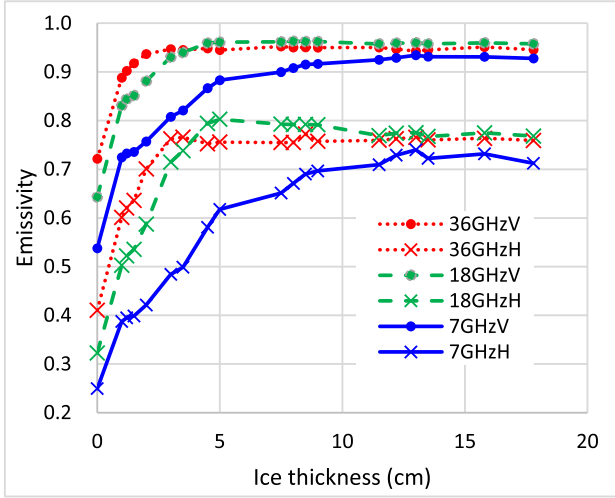


Fig. 5. Ice emissivity versus ice thickness for 7, 18, and 36 GHz.

TB18 Brightness temperature for 18 GHz;
V Vertical polarization;
H Horizontal polarization.

$$GR(36V18V) = (TB36V - TB18V) / (TB36V + TB18V) \quad (2a)$$

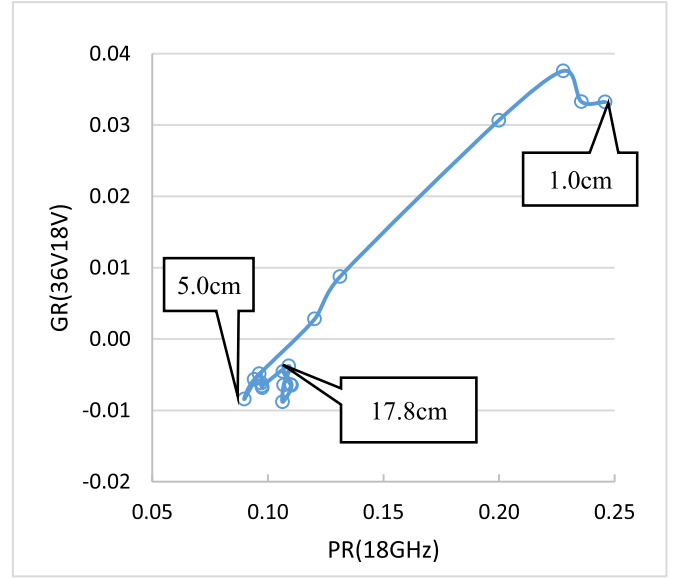


Fig. 6. PR versus GR for ice thickness 1.0–17.8 cm.

where

TB36 Brightness temperature for 36 GHz.

The scatterplots of PR versus GR were plotted in Fig. 6. Since the ice concentration of the target area in the ice tank was always 100%, it is natural to see the general trend of PR and GR gradually decreased as the ice thickness increased. On the other hand, GR showed a strange increase in the beginning of ice formation. Also, after the ice thickness of 5.0 cm, both PR and GR showed some irregular behavior. Some sea ice surface condition changes during the experiment could be the reason. We may need more experiments to identify those reasons.

In addition to 18 GHz, we also calculated PR for 7 and 36 GHz as follows:

$$PR(7 \text{ GHz}) = (TB7V - TB7H) / (TB7V + TB7H) \quad (1b)$$

where

TB7 Brightness temperature for 7GHz.

$$PR(36 \text{ GHz}) = (TB36V - TB36H) / (TB36V + TB36H). \quad (1c)$$

PR versus ice thickness was plotted for the three frequencies in Fig. 7 with ice thickness less than 20 cm. Though the vertical axis of Figs. 4 and 7 is upside down, the curve looks similar for each frequency, and both brightness temperatures and PR are saturated at almost the same ice thickness.

As for comparing the relationship between GR and ice thickness, we have also calculated GR for 36 and 7 GHz as follows:

$$GR(36V7V) = (TB36V - TB7V) / (TB36V + TB7V). \quad (2b)$$

GR versus ice thickness was plotted in Fig. 8 with a ice thickness of less than 20 cm. The curve of GR looks similar to the curve of PR, as shown in Fig. 7. Both graphs suggested the possibility of estimating ice thickness for less than 13.5 cm with PR (7 GHz) and GR (36V7V). However, we could not find a clear advantage against brightness temperatures measured with 7 GHz.

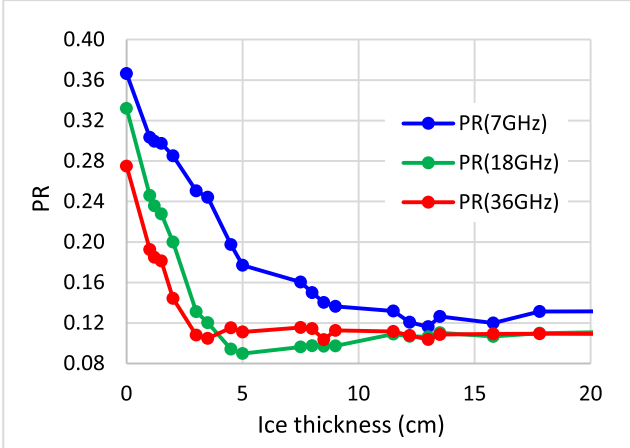


Fig. 7. PR versus ice thickness for 7, 18, and 36 GHz.

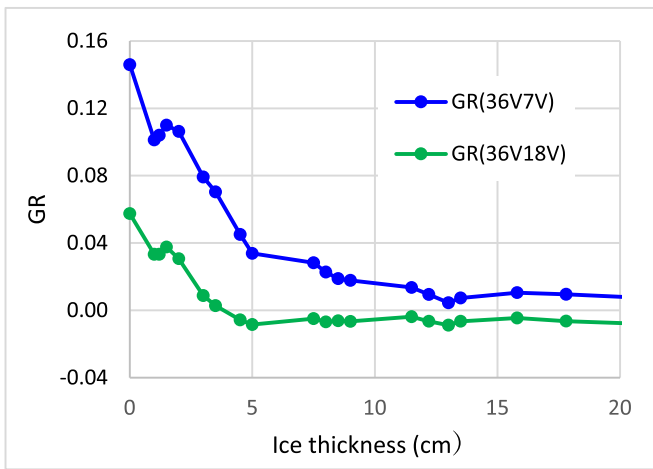


Fig. 8. GR versus ice thickness for ice thickness 0–17.8 cm.

B. Salinity Versus Ice Thickness

In order to examine the relationship between ice thickness and salinity, after each microwave brightness temperature measurement, ice samples were taken and melted, and bulk salinity was measured. Fig. 9 shows the relationship between the salinity and the thickness of ice. The salinity of seawater was 32.5 ppt and the salinity of the sea ice dropped sharply to 21.5 ppt when the sea ice thickness grew to 1.2 cm. Then, the salinity gradually declined as the sea ice grew, and the salinity became 11.1 ppt at the ice thickness of 11.5 cm. Over the ice thickness of 11.5 cm, the salinity was almost constant. This means that the ice salinity almost did not decline from 11.1 ppt even though the ice thickness grew over 11.5 cm. The possible reason why the minimum salinity value measured for ice thicknesses greater than about 11 cm was 11.1 ppt could be the limited volume of water in the tank hindered the expulsion of salt from the ice. However, we may need some more experiments to clarify the reason for this phenomenon.

There are several regression models proposed for fitting the relationship between salinity and ice thickness. Cox and Weeks [27] introduce the following simple linear equation:

$$S = 14.14 - 19.39h; \quad h \leq 0.4 \text{ m.} \quad (3)$$

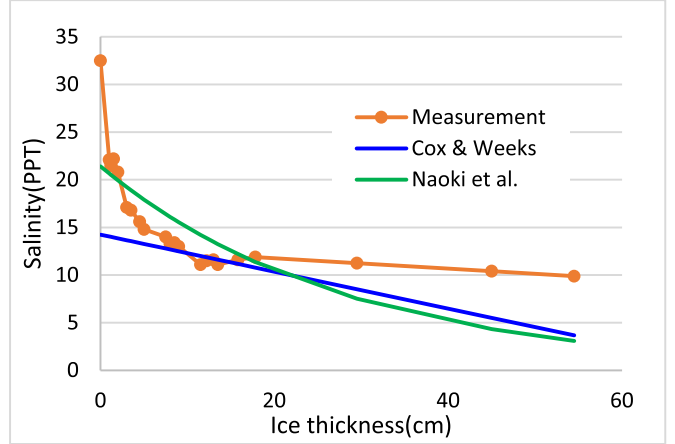


Fig. 9. Salinity versus ice thickness.

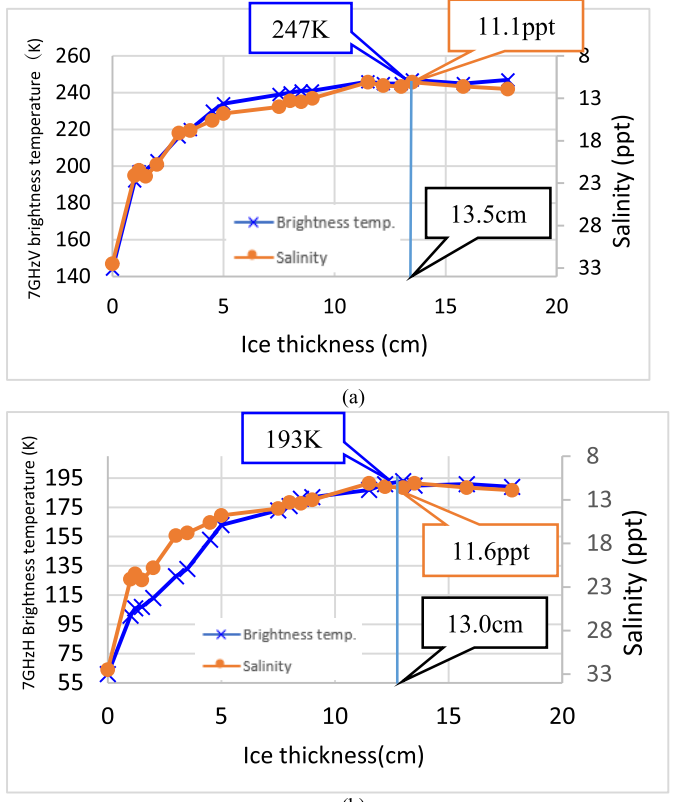


Fig. 10. 7-GHz brightness temperature versus ice thickness versus salinity. (a) V polarization. (b) H polarization.

Naoki et al. [20] generated an exponential equation as follows:

$$S = \exp(-3.55h + 3.06358) \quad (4)$$

where

S salinity;

h ice thickness in meter.

The two equation curves are plotted in Fig. 9 in comparison with the measurement data. However, neither of the equations matched the measurement data. Introducing bias to the exponential equation is one possibility of fitting the model to the experimental data. We may need more experiments,

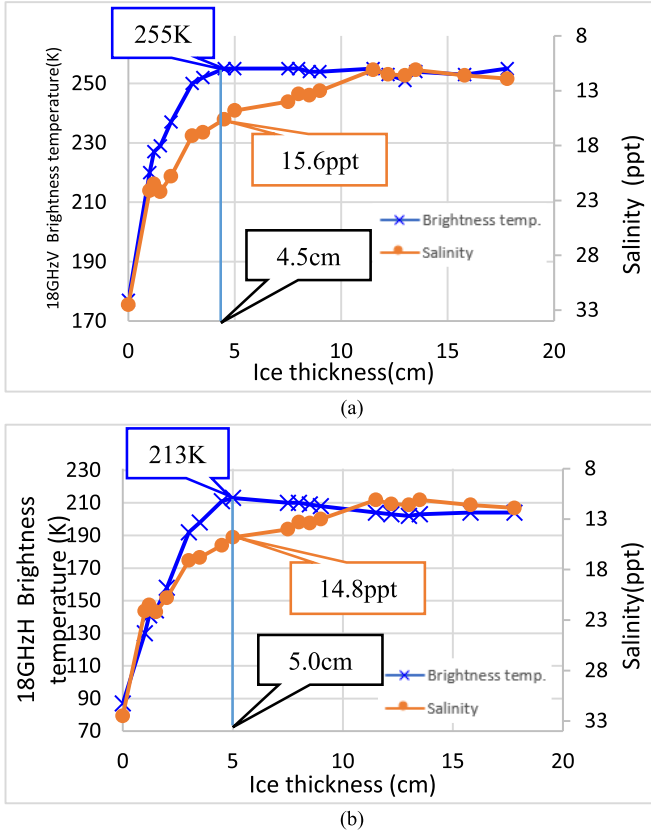


Fig. 11. 18-GHz brightness temperature versus ice thickness versus salinity. (a) V polarization. (b) H polarization.

including the measurement for thicker ice to improve the model.

C. Brightness Temperature/Emissivity Versus Salinity Versus Ice Thickness

Finally, we have examined the relationship between microwave brightness temperature, salinity, and ice thickness. Figs. 10–12 show the relationship of the three. Since the brightness temperature became almost constant after the ice thickness of around 15.0 cm as shown in Fig. 4, the graphs were made for the ice thickness of less than 17.8 cm to examine the detailed behavior of the three parameters. In these graphs, the x-axis is ice thickness, the y-axis on the left side is brightness temperature, and the y-axis on the right side is salinity. However, it should be noted that the salinity has been set upside down. The scale of ice thickness and salinity is the same for all the figures, but the scale of brightness temperature is scaled to adjust with the graph curve of salinity.

If we compare the graphs of Figs. 10–12, the graph curve of brightness temperature and salinity against ice thickness is quite similar. This strongly suggests that salinity is the main driving force of brightness temperature change against ice thickness. In other words, it is most likely because salinity declines as the ice grows, brightness temperature of ice increases as the ice grows.

Let us look at the details of each graph. As for 7-GHz V polarization, the brightness temperature took a maximum value of 247 K at the ice thickness of 13.5 cm with a salinity

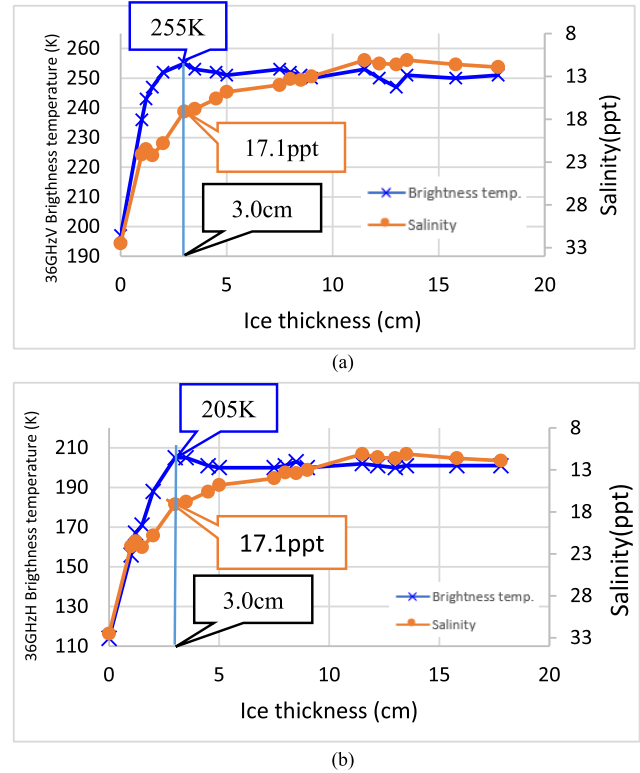


Fig. 12. 36-GHz brightness temperature versus ice thickness versus salinity. (a) V polarization. (b) H polarization.

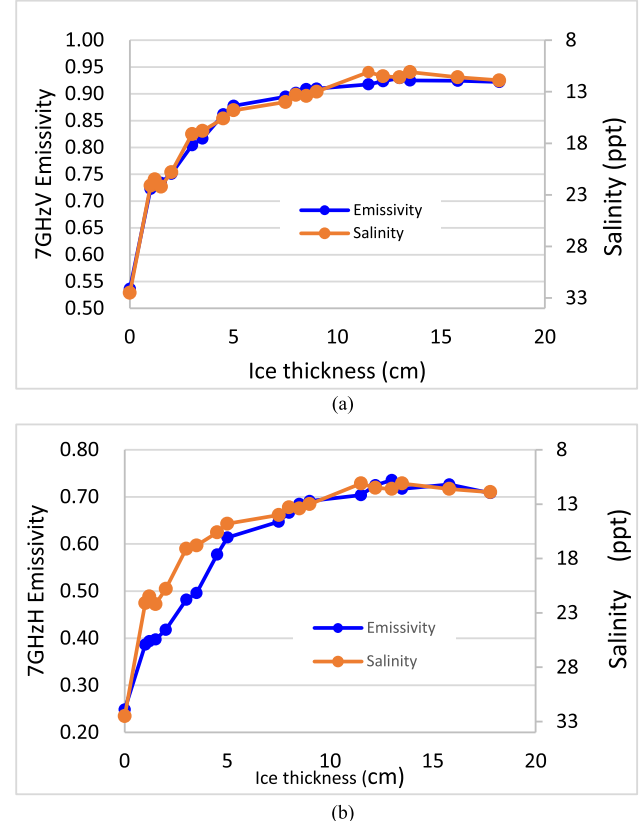
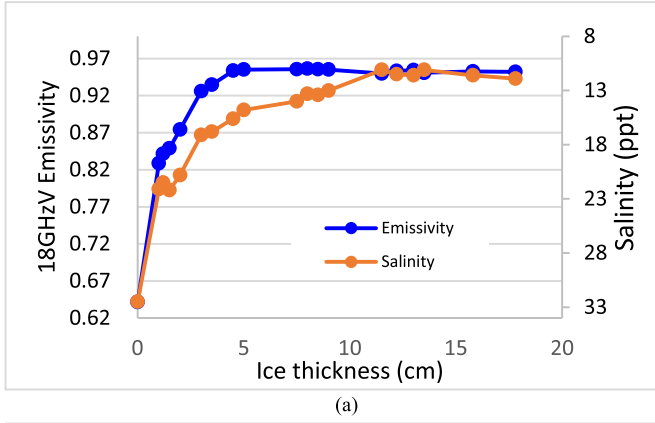
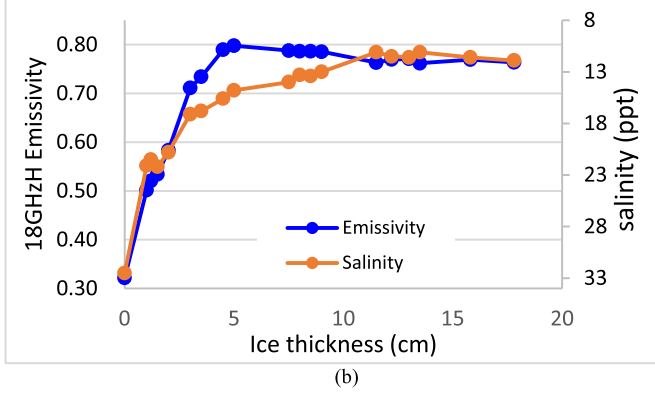


Fig. 13. 7-GHz emissivity versus ice thickness versus salinity. (a) V polarization. (b) H polarization.

of 11.1 ppt. As for 7-GHz H polarization, the brightness temperature took a maximum value of 193 K at the ice thickness of 13.0 cm with a salinity of 11.6 ppt. As for



(a)

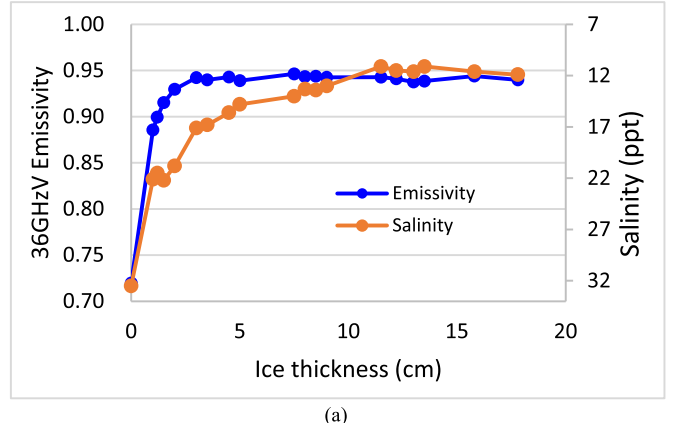


(b)

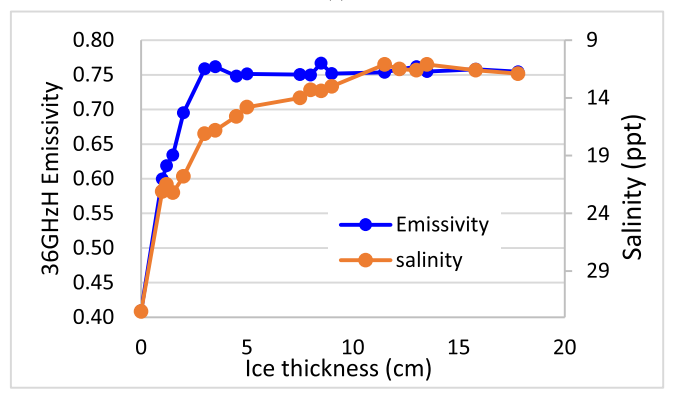
Fig. 14. 18-GHz emissivity versus ice thickness versus salinity. (a) V polarization. (b) H polarization.

36 GHz, the brightness temperature took a maximum value of 255 K for V polarization and 205 K for H polarization. However, the ice thickness was 3.0 cm and the salinity was 17.1 ppt for both polarizations. The result strongly suggests that lower frequencies are more sensitive to salinity and ice thickness than higher frequencies. Even though the salinity declined to 11.1 ppt at the ice thickness of 13.5 cm, the brightness temperature of 36 GHz V polarization reaches a maximum brightness temperature of 255 K at the salinity of 17.1 ppt with ice thickness of 3.0 cm, and the brightness temperature of 18-GHz V polarization reaches a maximum brightness of 255 K at 15.6 ppt with a ice thickness of 4.5 cm. These results suggest that in each frequency, certain limitation of detecting salinity exists and the values are lower at lower frequencies. Moreover, though the maximum brightness temperatures of V and H polarization were different for all three frequencies, the salinity at that point for V and H polarization was almost the same at each frequency. The results suggest that a certain limitation exists in estimating sea ice thickness using passive microwave radiometers at the higher frequencies of 18–37 GHz. On the other hand, the result of 7 GHz suggested the possibility of estimating the ice thickness in lower frequencies.

Various algorithms (such as [10], [11], [13], and [14]) are estimating ice thickness of more than 15 cm from satellite microwave observation data. Our results may give some negative impression to those algorithms. However, it should be noted that our study is focused on simulated bare ice. The conditions of real sea ice observed from satellites are more



(a)



(b)

Fig. 15. 36-GHz emissivity versus ice thickness versus salinity. (a) V polarization. (b) H polarization.

complex. Investigating how the sea ice surface conditions, such as snow cover, rainfall, and surface melting, are affecting the microwave brightness temperature measurement is important.

As references, the relationship between emissivity, salinity, and ice thickness are also shown in Figs. 13–15. If we compare Figs. 10–12 with Figs. 13–15, the graph curves of emissivity at each frequency are almost the same as that of brightness temperature. The smooth shape of each graph curve suggests the stability of the surface condition of sea ice during the experiment.

V. CONCLUSION

Sea ice desalination during growth due to brine expulsion is a well-known phenomenon. Since the desalination of sea ice increases the emissivity of sea ice, estimating sea ice thickness with the brightness temperature of sea ice measured by microwave radiometers seems to be reasonable. However, the question is how far the ice thickness information can be reflected in the brightness temperature measured by microwave radiometers. In this article, the authors have examined the basic relationship between microwave brightness temperature/emissivity, salinity, and thickness of simulated bare sea ice acquired with a tank experiment. The brightness temperature was measured by potable microwave radiometers saturated at a sea ice thickness of 3.0 cm with a salinity of 17.1 ppt for 36 GHz, 5.0 cm with a salinity of 14.8 ppt for 18 GHz, and 13.5 cm with a salinity of 11.1 ppt for 7 GHz. These

results suggested the limitation and possibility of estimating bare ice thickness from microwave observation. It may be quite difficult to estimate ice thickness of more than 5.0 cm with a microwave radiometer of higher than 18-GHz frequency. On the other hand, microwave radiometer observation with lower than 7-GHz frequency may have the possibility of estimating sea ice thickness of more than 13.5 cm. The experimental results strongly suggested that desalination plays the main role in increasing brightness temperature at the initial stage of ice growth, and the brightness temperature saturates at a certain salinity according to the frequency of a microwave radiometer. Our next step is to continue our sea ice experiment using our tank system and perform more precise measurements for sea ice thicker than 20 cm. Moreover, as Shokr et al. [21], [22] mentioned, microwave radiation from thin ice is particularly sensitive to surface change due to meteorological factors such as rain, freezing rain, slash, and snowfall. Evaluating the influence of those factors on the ice thickness estimation is also very important.

The final target of this study is to investigate the possibility of estimating sea ice thickness using satellite passive microwave radiometers such as AMSR2. However, the most challenging thing is to get the precise thickness of sea ice that corresponds to the footprint size of AMSR2. Airplane experiments may be a more realistic approach for the next step of our study.

ACKNOWLEDGMENT

The authors' support from Misako Kachi and Dr. Rigen Shimada of JAXA was very helpful. They would like to thank Hokkaido University of Education for kindly allowing them to set up the sea ice tank on the top of the university building and operate the facility. Finally, they also would like to thank all the reviewers for their productive comments. They were quite encouraging and were necessary to improve their paper.

REFERENCES

- [1] D. J. Cavalieri, P. Gloersen, and W. J. Campbell, "Determination of sea ice parameters with the NIMBUS 7 SMMR," *J. Geophys. Res., Atmos.*, vol. 89, no. 4, pp. 5355–5369, 1984.
- [2] J. C. Comiso, *SSM/I Sea Ice Concentrations Using the Bootstrap Algorithm*. Greenbelt, MD, USA: NASA Center for AeroSpace Information, 1985.
- [3] J. C. Comiso and K. Cho. (2013). *Description of GCOM-W1 AMSR2 Sea Ice Concentration Algorithm, Descriptions of GCOM-W1 AMSR2 Level 1R and Level 2 Algorithms*. JAXA Description of GCOM-W1 AMSR2 Sea Ice Concentration Algorithm, Descriptions of GCOM-W1 AMSR2 Level 1R and Level 2 Algorithms. JAXA NDX-120015A. [Online]. Available: http://suzaku.eorc.jaxa.jp/GCOM_W/data/doc/NDX-120015A.pdf
- [4] G. Spreen, L. Kaleschke, and G. Heygster, "Sea ice remote sensing using AMSR-E 89-GHz channels," *J. Geophys. Res., Oceans*, vol. 113, no. C2, Feb. 2008, Art. no. C02S03, doi: [10.1029/2005jc003384](https://doi.org/10.1029/2005jc003384).
- [5] J. C. Comiso and F. Nishio, "Trends in the sea ice cover using enhanced and compatible AMSR-E, SSM/I, and SMMR data," *J. Geophys. Res., Oceans*, vol. 113, no. C2, pp. 1–22, Feb. 2008.
- [6] J. C. Comiso, C. L. Parkinson, R. Gersten, and L. Stock, "Accelerated decline in the Arctic sea ice cover," *Geophys. Res. Lett.*, vol. 35, no. 1, Jan. 2008, Art. no. L01703.
- [7] J. C. Stroeve, M. C. Serreze, M. M. Holland, J. E. Kay, J. Malanik, and A. P. Barrett, "The Arctic's rapidly shrinking sea ice cover: A research synthesis," *Climatic Change*, vol. 110, nos. 3–4, pp. 1005–1027, Feb. 2012.
- [8] IPCC. (2021). *Sixth Assessment Report; Summary for Policy Makers*. [Online]. Available: https://www.ipcc.ch/report/ar6/wg1/downloads/report/IPCC_AR6_WGI_SPM_final.pdf
- [9] G. A. Maykut, "Energy exchange over young sea ice in the central Arctic," *J. Geophys. Res., Oceans*, vol. 83, no. C7, pp. 3646–3658, Jul. 1978.
- [10] K. Tateyama, H. Enomoto, T. Toyota, and S. Uto, "Sea ice thickness estimated from passive microwave radiometers," *Polar Meteorol. Glaciol.*, vol. 16, pp. 15–31, Jan. 2002.
- [11] S. Martin, R. Drucker, R. Kwok, and B. Holt, "Estimation of the thin ice thickness and heat flux for the Chukchi Sea Alaskan Coast Polynya from special sensor microwave/imager data, 1990–2001," *J. Geophys. Res., Oceans*, vol. 109, no. C10, pp. 1–10, Oct. 2004, doi: [10.1029/2004jc002428](https://doi.org/10.1029/2004jc002428).
- [12] S. Martin, R. Drucker, R. Kwok, and B. Holt, "Improvements in the estimates of ice thickness and production in the Chukchi Sea polynyas derived from AMSR-E," *Geophys. Res. Lett.*, vol. 32, no. 5, Mar. 2005, Art. no. L05505.
- [13] T. Tamura, K. I. Ohshima, T. Markus, D. J. Cavalieri, S. Nihashi, and N. Hirasawa, "Estimation of thin ice thickness and detection of fast ice from SSM/I data in the Antarctic Ocean," *J. Atmos. Ocean. Technol.*, vol. 24, no. 10, pp. 1757–1772, Oct. 2007.
- [14] G. Aulicino, G. Fusco, S. Kern, and G. Budillon, "Estimation of sea-ice thickness in Ross and Weddell seas from SSM/I brightness temperatures," *IEEE Trans. Geosci. Remote Sens.*, vol. 52, no. 7, pp. 4122–4140, Jul. 2014.
- [15] H. Kashiwase, K. I. Ohshima, Y. Fukamachi, S. Nihashi, and T. Tamura, "Evaluation of AMSR-E thin ice thickness algorithm from a mooring-based observation: How can the satellite observe a sea ice field with nonuniform thickness distribution?" *J. Atmos. Ocean. Technol.*, vol. 36, no. 8, pp. 1623–1641, Aug. 2019.
- [16] K. Cho and K. Naoki, "Procedure of extracting thin ice areas in the sea of Okhotsk using MODIS data," *ISPRS Ann. Photogramm., Remote Sens. Spatial Inf. Sci.*, vol. 2022, pp. 319–324, May 2022, doi: [10.5194/isprs-annals-v-3-2022-319-2022](https://doi.org/10.5194/isprs-annals-v-3-2022-319-2022).
- [17] S. A. Arcone, A. J. Gow, and S. McGrew, "Microwave dielectric, structural, and salinity properties of simulated sea ice," *IEEE Trans. Geosci. Remote Sens.*, vols. GE-24, no. 6, pp. 832–839, Nov. 1986, doi: [10.1109/TGRS.1986.289697](https://doi.org/10.1109/TGRS.1986.289697).
- [18] T. C. Grenfell, D. L. Bell, A. W. Lohanick, C. T. Swift, and K. S. Germain, "Multifrequency passive microwave observation of saline ice grown in a tank," in *Proc. Int. Geosci. Remote Sens. Symp., 'Remote Sens., Moving Toward 21st Century'*, vol. 3, Sep. 1988, pp. 1687–1690, doi: [10.1109/IGARSS.1988.569561](https://doi.org/10.1109/IGARSS.1988.569561).
- [19] S. V. Nghiem et al., "Diurnal thermal cycling effects on microwave signatures of thin sea ice," *IEEE Trans. Geosci. Remote Sens.*, vol. 36, no. 1, pp. 111–124, Jan. 1998, doi: [10.1109/36.55322](https://doi.org/10.1109/36.55322).
- [20] K. Naoki, J. Ukita, F. Nishio, M. Nakayama, J. C. Comiso, and A. Gasiewski, "Thin sea ice thickness as inferred from passive microwave and in situ observations," *J. Geophys. Res., Oceans*, vol. 113, no. C2, pp. 1–11, Feb. 2008.
- [21] M. Shokr, K. Asmus, and T. A. Agnew, "Microwave emission observations from artificial thin sea ice: The ice-tank experiment," *IEEE Trans. Geosci. Remote Sens.*, vol. 47, no. 1, pp. 325–338, Jan. 2009.
- [22] M. Shokr and L. Kaleschke, "Impact of surface conditions on thin sea ice concentration estimate from passive microwave observations," *Remote Sens. Environ.*, vol. 121, pp. 36–50, Jun. 2012, doi: [10.1016/j.rse.2012.01.005](https://doi.org/10.1016/j.rse.2012.01.005).
- [23] B. J. Hwang, J. K. Ehn, D. G. Barber, R. Galley, and T. C. Grenfell, "Investigations of newly formed sea ice in the Cape Bathurst polynya: 2. microwave emission," *J. Geophys. Res., Oceans*, vol. 112, no. C5, May 2007, Art. no. C05003.
- [24] K. Naoki, M. Nakayama, T. Tanikawa, and K. Cho, "Preliminary results on the relationship between microwave brightness temperature and sea ice thickness acquired with a tank experiment," in *Proc. AGU Fall Meeting*, 2018, p. 1, Paper C31D-1567.
- [25] K. Naoki, M. Nakayama, T. Tanikawa, and K. Cho, "The microwave brightness temperature observation of growing thin sea ice in tank experiment," in *Proc. AGU Fall Meeting*, 2019, p. 1, Paper C51D-1330.
- [26] M. Nakayama, K. Naoki, T. Tanikawa, and K. Cho, "Development of a sea ice tank system for measuring microwave properties of sea ice," *J. Glaciol.*, vol. 2024, pp. 1–28, Jan. 2024.
- [27] G. F. N. Cox and W. F. Weeks, "Salinity variations in sea ice," *J. Glaciol.*, vol. 13, no. 67, pp. 109–120, 1974.



Kohei Cho was born in Tokyo, Japan, in 1955. He received the B.S. degree in applied physics from the Tokyo University of Science, Tokyo, in 1979, the M.S. degree in image engineering from Chiba University, Chiba, Japan, in 1981, and the Ph.D. degree in civil engineering from the University of Tokyo, Tokyo, in 1982.

After working with the Remote Sensing Technology Center (RESTEC), Tokyo, as a Researcher for ten years. In 1992, he joined Tokai University, Tokyo, where he is currently a Professor. He has been the General Secretary of the Asian Association on Remote Sensing (AARS), Tokyo, since 2009. His scientific interest mainly focused on sea ice remote sensing.

Dr. Cho is currently a member of the JAXA AMSR2 PI Team. He was awarded the Dr. Boon Indrambarya Gold Medal of AARS in 2009, the Samuel Gamble Award of ISPRS in 2012, and ISPRS Fellow in 2022.



Masashige Nakayama was born in Hokkaido, Japan, in 1974. He received the B.S. degree in applied science and the M.Ed. degree in education from the Hokkaido University of Education, Hokkaido, in 1997 and 1999, respectively, and the Ph.D. degree in engineering from Tokai University, Tokyo, Japan, in 2002.

From 2002 to 2004, he was a Researcher with the Japan Aerospace Exploration Agency (JAXA), Chofu, Japan. He is currently an Associate Professor with the Hokkaido University of Education. He performed the basic design and refinement of an experimental tank. He also contributed to radiometric observations. His research topics include passive microwave radiometry from sea ice and science education.



Kazuhiro Naoki was born in Kagoshima, Japan, in 1976. He received the B.S. degree in applied science and the M.Ed. degree in education from the Hokkaido University of Education, Hokkaido, Japan, in 2000 and 2002, respectively, and the Ph.D. degree in science from Chiba University, Chiba, Japan, in 2007.

From 2009 to 2014, he was a Researcher with the Japan Aerospace Exploration Agency (JAXA), Chofu, Japan. He has been working with Tokai University Research and Information Center, Tokyo, Japan. He is currently in charge of research and development. He contributed to in situ observations of sea ice.



Tomonori Tanikawa was born in Hokkaido, Japan, in 1976. He received the B.S. degree in applied science from the Hokkaido University of Education, Hokkaido, in 2000, and the M.S. and Ph.D. degrees in life and environmental science from the University of Tsukuba, Tsukuba, Japan, in 2002 and 2005, respectively.

From 2005 to 2015, he was a Researcher with the Kitami Institute of Technology, Kitami, Japan; the Stevens Institute of Technology, Hoboken, NJ, USA; and the Japan Aerospace Exploration Agency (JAXA), Chofu, Japan. Since 2015, he has been working with the Meteorological Research Institute, Tsukuba, Japan, where he is currently a Senior Researcher. His research interests include the development of optical/microwave radiative transfer models of snow/sea ice surfaces and their application to the satellite remote sensing of the cryosphere.